IOP PUBLISHING JOURNAL OF PHYSICS: CONDENSED MATTER

J. Phys.: Condens. Matter **19** (2007) 113102 (25pp) doi:10.1088/0953-8984/19/11/113102

TOPICAL REVIEW

Confocal microscopy of colloids

V Prasad, D Semwogerere and Eric R Weeks

Department of Physics, Emory University, Atlanta, GA 30322, USA

E-mail: vprasad@physics.emory.edu

Received 5 September 2006, in final form 5 January 2007
Published 27 February 2007
Online at stacks.iop.org/JPhysCM/19/113102

Abstract

Colloids have increasingly been used to characterize or mimic many aspects of atomic and molecular systems. With confocal microscopy these colloidal particles can be tracked spatially in three dimensions with great precision over large time scales. This review discusses equilibrium phases such as crystals and liquids, and non-equilibrium phases such as glasses and gels. The phases that form depend strongly on the type of particle interaction that dominates. Hard-sphere-like colloids are the simplest, and interactions such as the attractive depletion force and electrostatic repulsion result in more non-trivial phases which can better model molecular materials. Furthermore, shearing or otherwise externally forcing these colloids while under microscopic observation helps connect the microscopic particle dynamics to the macroscopic flow behaviour. Finally, directions of future research in this field are discussed.

(Some figures in this article are in colour only in the electronic version)

Contents

1. Introduction

Optical microscopy is widely used in many systems where the domain of interest lies in the submicrometre to micrometre range. These include biological systems such as cells or tissue as well as areas of 'soft' physics such as complex fluids and colloidal dispersions, the main focus of this review. Since the important length scales are of the order of the wavelength of visible light, microscopy provides a powerful tool to obtain real-space and real-time information about the complex mechanisms that govern these systems [1]. The ease of sample preparation at room temperature and atmospheric pressure (as opposed to, say, low temperature or low pressure conditions for electron microscopy) also makes optical microscopy a convenient technique. Nevertheless, certain problems exist for complex many-body systems that interact with light; the most prominent one being multiple scattering. Visualization deep within the sample is difficult for an optically dense sample such as a biological tissue or a concentrated colloidal dispersion, as the light that enters the sample undergoes many scattering events resulting in blurriness of the image.

This problem was first faced by Marvin Minsky in the 1950s as he tried to visualize the way nerve cells were connected in the human nervous system [2]. His solution was two-fold: first, point by point illumination of the sample to minimize aberrant rays of scattered light from regions outside the image plane of interest; and second, a pinhole aperture in the image plane on the other side of the objective, to reject out-of-focus light. This prototype for the first confocal microscope used a carbon-arc lamp as the light source and a translating stage to visualize each point of the sample. Subsequent improvements utilize a laser and scan the laser beam rather than translating the sample. These two improvements enabled confocal microscopy to become a powerful tool for many scientific fields [3–5]; details of these improvements, as well as advances in the speed and resolution of confocal imaging, are described in later sections of this review.

The use of confocal microscopy in colloidal systems is a relatively recent development, in part driven by the discovery that monodisperse colloids could mimic many of the phases seen in atomic systems [6]. While these observations were performed by bulk techniques such as light scattering, further information about the microscopic details of these systems required visualization in concentrated dispersions. One of the first studies to look at colloids with a confocal microscope was by Yoshida *et al* in 1991 [7] who looked deep within a sample of charged polystyrene latex colloids and observed hexagonal ordering of the spheres. van Blaaderen and Wiltzius [8] extended the capability of confocal microscopy to denser systems, imaging spheres with packing fractions of $\sim$60% to observe structure in the so-called colloidal glass phase. Such a high density of particles required a significant advance in image-analysis algorithms; the positions of thousands of particles separated by distances slightly larger than their diameter had to be located to high accuracy. Once this was achieved almost any micrometre-sized colloidal system could be studied by confocal microscopy.

Advances in imaging and particle-tracking have led to rapid advances in our understanding of colloidal phenomena, and confocal microscopy is currently a tool in the laboratories of many research groups. In subsequent sections we discuss the details of how confocal microscopes function and some of the interesting physics governing colloidal systems that can be captured with this technique.

2. Properties of colloids

2.1. Hard spheres and their phase behaviour

Colloids have been used as models for atomic and molecular systems as they demonstrate many of the phases observed in such systems. The simplest model system is the hard-sphere system [9–13] in which the colloids are non-interacting at all separations beyond their radius and infinitely repulsive on contact. The sole control parameter that determines the phase behaviour of hard-sphere colloids is the sphere volume fraction ϕ, a non-dimensional quantity related to the number density n ($\phi = (4\pi/3)a^3 n$ with particle radius a). Here we discuss only the simple monodisperse case, although other parameters that could be considered include polydispersity, the aspect ratio of ellipsoids, etc. The size of the sphere is not a control parameter for ideal hard spheres, but for colloidal suspensions it can strongly affect sedimentation or even the overall dynamics of the sphere. In the case of sedimentation this is because gravitational energy is still significant at the colloidal length scale when compared to thermal fluctuations. Balancing this energy with $k_B T$ gives a gravitational height $h = k_B T/F_g$, where the gravitational force on a sphere of radius a is $F_g = (4/3)\pi a^3 \Delta\rho g$ ($\Delta\rho$ is the density difference between the colloid and the surrounding fluid). The gravitational height can be varied by many orders of magnitude, either by going to a low gravity environment, such as in space [14], or a high gravity one, by mismatching the density of the colloid and solvent [15–17]. For most systems it is desirable to have h larger than the sample chamber height as gravitational effects can then be neglected (for example, $h = 1$ mm for $a \sim 0.5$ μm and $\Delta\rho = 1$ kg m^{-3}). The other effect of size arises due to diffusion; larger particles diffuse more slowly than smaller particles. This can be quantified by the diffusion coefficient $D = k_B T/6\pi\eta a$ which determines how fast a sphere diffuses in a fluid solvent of viscosity η. The time scale for a particle to diffuse a distance equal to its own radius is $\tau_B = a^2/6D$; this sets the dynamic time scale of the colloidal system in question (for a micrometre-sized particle in water τ_B is of the order of seconds).

In a dilute system ($\phi \to 0$) the spheres are disordered and generally far from each other like a dilute gas. As the volume fraction increases from the dilute limit spheres remain in a disordered state. Denser states have spatial correlations between the positions of the spheres and thus these states are more analogous to liquids than to gases, although this distinction is somewhat arbitrary. The maximum amorphous packing is $\phi \approx 0.64$ [18–21], often termed RCP for 'random close packing' (see figure 1).

If the hard-sphere system is allowed to equilibrate as the volume fraction is increased, however, the system undergoes an entropy driven phase transition to a crystalline state [6]. This transition starts at $\phi = 0.494$ with a coexistence region up to $\phi = 0.545$. States with $0.494 < \phi < 0.545$ have crystalline domains ($\phi = 0.545$) coexisting with liquid regions ($\phi = 0.494$) (see figure 1). This phase persists from $\phi = 0.545$ to 0.740, the maximal packing a 3D system of monodisperse spheres can obtain.

In addition to these equilibrium phases colloidal systems can also exhibit non-equilibrium behaviour. For example, at $\phi = 0.58$ the crystallization of the colloids can be arrested by the appearance of a metastable, kinetically trapped state known as a glass that persists until

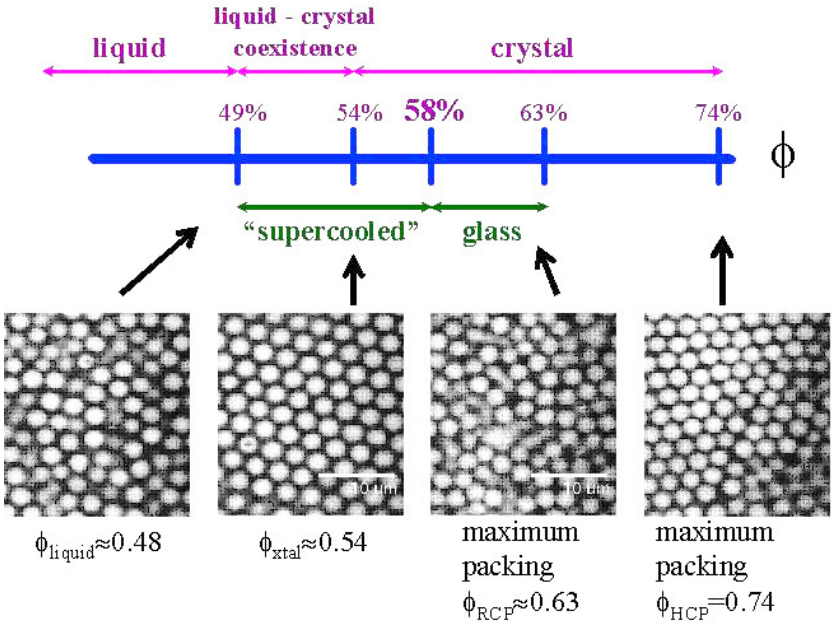

Figure 1. Phase diagram of hard spheres, where the control parameter is the volume fraction ϕ.

random close packing. (It is now believed that this requires some slight polydispersity to occur, ∼5% [22, 23].) The glass is characterized by a large increase in the viscosity of the system [24] despite no perceptible change in structure [8]. Furthermore, the colloidal glass has some properties of a solid: for example, the system has a finite yield stress, and the elastic modulus is larger than the viscous modulus [25]. While the glass transition has also been observed in atomic and molecular systems, the mechanism that drives this transition is still a matter of active research [26–29].

Confocal microscopy experiments studying hard-sphere like colloidal particles are discussed in section 5.

2.2. Attractive and repulsive interactions

Hard spheres are imperfect as models for atoms. Real materials have chemical attractions and bonds that help hold the atoms together, as well as repulsive interactions between their nuclei that stabilize them. Thus, it is critical to study colloids with more complex interactions (attractive and repulsive) than the simple hard-sphere short-range repulsion. While this increases the parameter space to be explored, there is also more richness in the observed phase behaviour. Here we offer only brief descriptions of four important interactions: steric stabilization, Coulombic repulsion, van der Waals attraction and depletion. For more information see [30–32].

Steric stabilization occurs when a boundary layer is added to a colloidal particle. For example, some colloids have a layer of short polymers coating the surface and sticking out [33]. If two such particles approach, the polymers begin overlapping and obstructing each other; this is a repulsive interaction and prevents the colloids from approaching too closely. It is precisely such colloids that are most often used as model hard spheres [8, 34]. In other colloidal suspensions, most typically in aqueous suspensions, adding a surfactant serves the

same purpose. The hydrophobic tail of the surfactant coats the colloidal particles, and the polar head sticks into the water, thus providing the steric stabilization.

Coulombic repulsion occurs when surface groups on the colloidal particles dissociate, leaving the particles charged. Counterions in the water hover nearby, forming an electrostatic 'Debye double layer' around the particle. Particles separated by distances much larger than the thickness of the Debye double layer feel essentially no electrostatic repulsion. By adding salt, the length of the Debye double layer can be reduced. The details of the interaction between the charged colloidal particles and their counterions are complex; for more details see [30–32]. Interesting phases seen with charged particles are discussed in section 6.4.

While repulsive forces prevent colloidal aggregation, and are thus often of industrial and commercial interest, attractive interactions are often desirable as more closely modelling atomic interactions. The van der Waals force is caused by fluctuating dipoles in the colloidal particles. The interaction potential is short-ranged, decaying as $1/r^6$, but is very strong at short distances, with energies of interaction $U \gg k_B T$. Particles which are not sterically stabilized or charge stabilized can approach each other at close distances and tend to stick irreversibly due to the van der Waals force [30, 32]. This force can be diminished somewhat by using a solvent having the same refractive index as the colloidal particles.

The depletion force arises in the presence of a polymer or smaller species of colloid. The smaller entities create an osmotic pressure within the solvent that drives the large colloids together. The depth of the interaction can be changed by changing the polymer (small colloid) concentration while the range of the interaction can be varied by varying the size of the polymer (smaller colloid) [35–37]. The ability to change depth and range independently is the key advantage of the depletion force for studies of model systems. Typically the size of the smaller species is limited to at most $\approx$10% of the large particles.

Studies of colloids with attractive interactions are discussed in section 6.1. In general, understanding how the microscopic details of particle interactions relate to their mesoscopic structure and macroscopic rheological properties [32] is one of the principal questions of the field of soft condensed matter, and is highly relevant to industrial use of soft materials.

A brief mention should be made of the most commonly used colloids, polymethylmethacrylate (PMMA) spheres of radius $a = 0.2$–2 μm coated with a sterically stabilizing agent that prevents aggregation [33]. Particles are dyed by introducing a fluorophore into the spheres, either after swelling them or else when the colloids are originally synthesized [38–40]. Some groups are partial to using silica spheres that have a fluorescent core [41]. While PMMA spheres can easily be suspended in solvents that match them for index and density, recent studies have shown that the colloids have a slight charge on them, which changes the inter-particle potential from hard-sphere-like to soft [42]. Silica spheres, escaping most of the effects of charge, cannot be easily density matched. The choice of colloid, therefore, depends on the details of the system to be studied and the relative importance of interaction potential versus density matching.

3. Comparison of techniques to study colloidal suspensions

The size ($\sim\mu$m) and energy scale ($\sim k_B T$) of colloidal particles decides the techniques used to study such suspensions. These techniques typically fall into three categories: scattering, rheology and microscopy. Each of these techniques has distinct advantages and disadvantages, which we describe in detail below.

Scattering is the process where radiation incident on the sample is deflected from its trajectory. Measuring the intensity of scattered radiation as a function of scattered angle and time gives information about the structure and dynamics of the sample. Typically, the

types of radiation used are neutrons [43–47], x-rays [48–51] or laser light in the visible spectrum [52–56]. Since the optimum size of colloidal particles lies near the visible spectrum of light, laser light scattering is easily the most popular of these techniques [25]. Light scattering can be further subdivided into two broad categories: static and dynamic scattering. Static light scattering involves measuring the intensity of scattered light at different scattering wave vectors q ($q = 4\pi n/\lambda \sin(\theta/2)$, where λ is the wavelength of incident light and θ is the scattering angle). In this way, the structure of colloidal suspensions can be measured at different wave vectors and hence different length scales. Dynamic light scattering, on the other hand, measures the fluctuation of the scattered intensity of light, and therefore provides information about the motion of the particles in the suspension. Measuring the dynamics at different q-vectors provides information about local or collective motions in the suspension. Because light scattering averages over large ensembles of the system configurations, it provides highly accurate measurements of both structure and dynamics. However, because of this ensemble average, it also fails to accurately probe local properties. For example, light scattering can accurately measure the fraction of a colloidal sample which is crystalline, but not determine the shapes of individual crystalline domains. Another disadvantage of light scattering is its reliance on single scattering events. For relatively turbid samples, multiple scattering causes decoherence of the incident beam, and therefore lack of information about structure and dynamics present in the sample. Certain techniques such as two-colour light scattering [57–60] attempt to circumvent this problem by using two incident beams with the same q-vector but different scattering geometries. Cross-correlating the two scattered beams gives information mainly about single scattering events, as multiply scattered events are uncorrelated. Other techniques such as diffusing-wave spectroscopy [61–64] use the property of multiple scattering by assuming that light traversing the sample behaves like a random walk. The change in phase of the beam as it traverses the sample is related to dynamical processes such as particle motions or rearrangements. However, optical microscopy is still superior to these techniques in terms of providing quantitative information about local events.

Rheology is the study of deformation and flow of a material in response to an external perturbation, such as an applied force or thermal fluctuations. Most colloidal systems are viscoelastic, that is, they have both elastic and viscous responses to such perturbations. Typically, the elastic response of a colloidal suspension is described by its elastic modulus, which has the same dimensions as energy density. Therefore, a crude estimate of the magnitude of the elastic modulus can be given by $k_{\mathrm{B}}T/a^3$, which is of the order of 1 Pa. The viscous response, on the other hand, is set by the viscosity of the background solvent, and is typically of the order of 1 mPa s and higher. The complex rheological behaviour of colloidal suspensions arises from the coupling between the colloidal particles (or the networks and aggregates they form) and the solvent around them [65, 66]. Conventional rheometers are capable of measuring the bulk viscoelasticity of colloidal fluids [67], glasses [68] and gels [66, 69, 70]. Since these measurements are macroscopic in nature, the structure and dynamics at short length scales can only be indirectly inferred. This is usually done by comparison with a theoretical microscopic model, or complementary microscopic measurements by optical methods.

Conventional optical microscopy can easily resolve individual colloidal particles of size $\sim$1 μm, which is of order the wavelength of visible light. Further, because of its relative ease of use and low cost, microscopy is a popular tool for the study of colloidal suspensions [1]. The most common and basic mode of operation of a conventional microscope is bright field, where objects appear dark under bright illumination. For most colloidal suspensions, this method provides images of adequate quality, but since the particles are nearly transparent by virtue of index matching, these images usually display poor contrast. Other techniques such as phase contrast [71, 72] or differential interference contrast (DIC) microscopy [73] can be

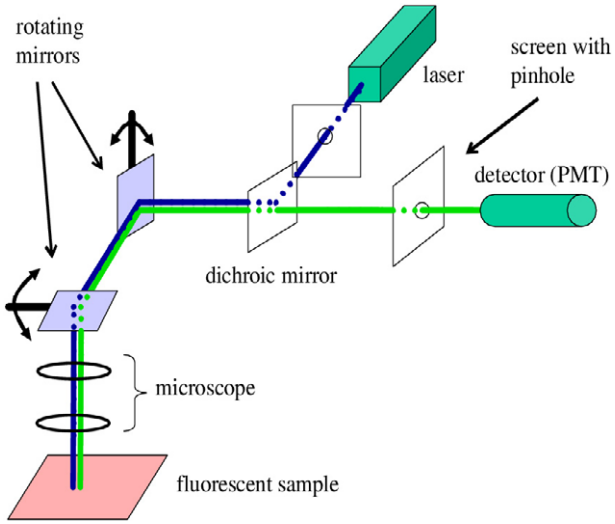

Figure 2. Schematic diagram of a conventional confocal microscope. The screen with the pinhole lies in the back focal plane of the sample with respect to the objective, thus rejecting most out-of-focus light. The rotating mirrors scan the sample pixel by pixel, and are the rate-limiting step for obtaining an image.

used to enhance the contrast of such images. An extensive description of conventional optical microscopy of colloids is beyond the scope of this review; an excellent article on this topic and related techniques is provided by Elliott and Poon [74]. However, conventional microscopy suffers from the same problem as light scattering, namely multiple scattering from objects that are out of focus within the illuminated region prevents imaging deep within a sample. Further, if care is not taken, optical microscopy can lead to the observation of certain artefacts [75] which in turn leads to incorrect physical interpretation of the system in question.

Confocal microscopy provides a way to overcome many of the problems caused by multiple scattering or low contrast images, the subsequent section details the internal workings of a confocal microscope as well as its resolution and speed limitations.

4. How a confocal microscope works

A laser scanning confocal microscope (LSCM) incorporates two principal ideas: point by point illumination of the sample and rejection of out of focus light [3–5]. Figure 2 shows the internal workings of a confocal microscope. Laser light (blue line) is directed by a dichroic mirror towards a pair of mirrors that scan the light in x and y. The light then passes through the microscope objective and excites the fluorescent sample. The fluoresced (light green) light from the sample passes back through the objective and is descanned by the same mirrors used to scan the sample. The light then passes through the dichroic mirror through a pinhole placed in the *conjugate focal* (hence the term confocal) plane of the sample; the pinhole thus rejects all out-of-focus light arriving from the sample. The light that emerges from the pinhole is finally measured by a detector such as a photomultiplier tube.

At any particular instant only one point of the sample is observed; a computer reconstructs the 2D image plane one pixel at a time. A 3D reconstruction of the sample can be performed by combining a series of such slices at different depths. Figure 3 shows one such reconstruction of a sample consisting of PMMA spheres of diameter $d = 2$ μm. This 3D capability is one

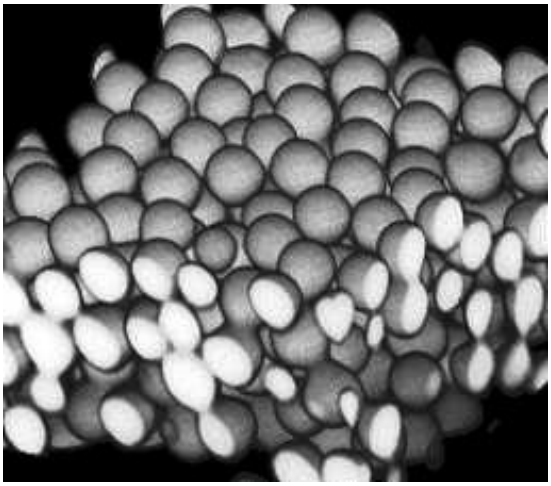

Figure 3. 3D reconstruction of a colloidal sample of PMMA spheres ($d = 2\ \mu$m).

of the main advantages to confocal microscopy. Another, related, advantage is that the pinhole filters out background fluorescence that would normally prevent clear imaging of a high volume fraction sample. It is precisely this 'sectioning' ability that allows a crisp image at a given depth into the sample that in turn enables the 3D imaging.

4.1. Resolution

Like a conventional optical microscope, the resolution of a confocal microscope is limited by diffraction of light. The image of an ideal point viewed through a circular aperture is blurred, and the diffracted image is known as an Airy disc. The size of the Airy disc depends on the wavelength of the laser source and the numerical aperture of the objective lens [3–5]. This Airy disc limits the maximum resolution of the microscope in the sample plane due to the Rayleigh criterion, which states that two Airy discs must be separated by at least their radius in order to be resolved. For the optical setup of most commercially available confocal microscopes this limit is about 200 nm. More generally, the Airy disc is the image of a perfectly focused point; an out-of-focus image tends to be even more blurred due to diffraction. The 3D generalization of the Airy disc function is termed the 'point-spread function'. Just as the intensity of light smoothly decreases away from the centre of the Airy disc in x and y, the intensity also decreases in z for the point spread function. Limitations in the optics make this decrease slower in z than in x or y and thus the z resolution is poorer, typically at best 500 nm [3–5]. (Note that in practice the size of the confocal pinhole is set to be the size of the Airy disc after it is magnified by the microscope optics. A larger pinhole allows too much out-of-focus light to pass through; a smaller pinhole degrades the signal to noise ratio.)

It is encouraging to notice that there is an important difference between resolution and 'ability to locate the position'. For a tiny and isolated fluorescent object, the position of that object can often be located to a precision better than the resolution. The image of the object will show up as a spatially extended Airy disc, and the 'centre of mass' of that round image can be found. If the disc is $\sim N$ pixels wide and each pixel is M micrometres across, the centre of the disc can be estimated to about M/N accuracy, which often beats the optical resolution. This is a useful trick, but is not solving the same problem as resolution. Resolution lets you decide whether you are looking at two closely positioned bright objects or just one big object.

In some cases various tricks can be performed to make the spot size bigger (increase N) so that the centre can be located to even higher precision.

The magnification is something different altogether. The technical definition compares the apparent angular size of the image to the actual angular size of the object as it would appear if it were 25 cm away from your eye [4]. This is a somewhat arbitrary definition. In reality, one often takes pictures using a CCD camera on a microscope and projects them on a monitor. Using a larger monitor can certainly magnify the image further, but it will still be just as blurry or sharp as the resolution. Thus, when considering how 'good' a microscope is, the most important question is what the resolution is. In general, high magnification lenses also have better resolutions. (More technically, a microscope objective's resolution is quantified by the numerical aperture; see [4] for details.)

4.2. Scanning speed

The speed of most confocal microscopes is limited by the rate at which the mirrors (see figure 2) can scan the entire sample plane. Typically this speed can range from 0.1 to 30 Hz. Until recently, standard confocal microscopes would use galvanometers to move the mirrors back and forth in a saw-tooth pattern. However, this is a slow process even for moderately sized images. For example, a 512 × 512 pixel image taken at video rates (30 frames s^{-1}) requires the galvanometer to scan a single direction at a frequency of $\sim 30 \times 512 = 15$ kHz, much faster than its operating specifications of a few kilohertz. Two designs are used to overcome this limitation and capture images at high speeds: (1) acousto-optic deflectors (AODs) and (2) Nipkow discs.

An AOD is a crystal that acts as an electronically tunable diffraction grating. Radio frequency sound waves are sent through the crystal and change the local refractive index. This sets up a standing wave pattern which acts as a diffraction grating to deflect the laser light. Therefore, changing the frequency and wavelength of the sound waves rapidly allows for quick and accurate steering of the laser beam. Because there are no moving parts the scanning is not limited by inertia, and so the speeds obtained with an AOD for a 512 × 512 pixel image can be as fast as 30 Hz. The main disadvantage of an AOD is that different wavelengths are deflected to different degrees. Since the excitation and the emitted light have different wavelengths, the AOD cannot be used to descan the light from the sample. This problem is partially resolved by descanning in one direction with a slow galvanometer and collecting the light with a slit rather than a pinhole. This reduces the amount of optical sectioning and slightly distorts the image due to the loss of circular symmetry. Nevertheless, it still produces high quality images (e.g. figure 3).

An even faster technique uses a Nipkow disc [3, 5, 76]. A Nipkow disc microscope creates an image by passing the laser light through a spinning mask of pinholes. The excitation light travels through the pinholes onto the sample and the fluoresced light returns through the same pinholes. The pinholes are arranged so that as the disc spins, they scan across every pixel in the sample. This full-image scan only requires the disc to spin perhaps 1/15th of a revolution; a rotation rate of 40 revolutions per second results in up to 600 frames s^{-1}. One disadvantage of the Nipkow disc, however, is that the pinhole size is fixed for a 100× oil objective which makes the technique less than optimum for lower magnifications. This is an issue when one obtains a wide field of view by going to lower magnifications. Another disadvantage is that large portions of the sample plane are illuminated simultaneously, increasing the background fluorescence. This problem becomes especially severe deep within the sample.

The time it takes a colloid ($a = 200$ nm) to diffuse its radius in water is of the order of $\tau_B = a^2(6\pi\eta a/k_B T) \sim 37$ ms. Therefore, even at the limits of resolution and scanning speeds

it is reasonable to expect accurate observations of thermal motion of colloidal particles with confocal microscopes.

Once the colloids have been visualized, the positions within an image or sequence of images can be found to sub-pixel accuracy [77–79]. If particles move less than their typical inter-particle spacing, then their locations between images can be connected and tracked over long periods of time. Typically confocal microscopy is used to study high volume fraction samples for which particle motion is inherently slower and thus more amenable to these tracking methods [78]. However, recent techniques allow particle tracking in the presence of rapid, non-uniform flow [80]. In general tracking can be done in either 2D or 3D; numerous examples of its use are given below.

5. Observations of hard-sphere colloids

5.1. Hard-sphere colloidal crystals

At volume fractions $0.494 < \phi < 0.545$ a hard-sphere colloidal suspension spontaneously phase separates into a crystalline and a liquid phase (see figure 1). The microscopic details of this phase separation are not only interesting in their own right, but also provide unique insights into the details of the nucleation dynamics and growth of solid state crystals. Since colloids are much larger, they can be observed in real space and real time, unlike atomic systems. Crystalline regions in 2D can be identified with the local bond orientational parameter ψ_6 [81]. This parameter, sensitive to hexagonal order where the nearest neighbours of a given particle are spaced roughly 60° apart, ranges from 0 to 1 ($\psi_6 = 1$ for a perfect hexagonal 2D crystal). Three-dimensional crystalline regions have been explored with bond orientational order parameters that assumes that two neighbouring particles with similar orientation of their neighbours are classified as ordered neighbours, and particles with eight or more ordered neighbours are identified as being crystal-like [82, 83].

The nucleation and growth of crystallites in a bulk system was observed in real time [84]. There are two competing factors for free energy that determine these growth rates, chemical potential and surface tension. The difference in chemical potential lowers this energy in the crystalline phase compared to the liquid phase, but the surface tension between the two phases increases it. For small crystalline regions surface tension dominates and the regions tend to shrink. Above a critical size, however, the regions grow as the chemical potential term (proportional to the volume) dominates the surface tension term (proportional to the surface area). These behaviours were observed using confocal microscopy and a critical size of roughly 60–100 particles measured [84], in agreement with computer simulations [85]. The structure of the post-critical crystallites was also determined, with nuclei found to be random hexagonal closed packed (rhcp) in agreement with crystal nuclei observed in computer simulations and light scattering measurements [34]. Finally, crystallites were found to be slightly non-spherical in shape, with rough interfaces with the fluid phase. This was considered to be indicative of a low surface tension ($\gamma \sim 10^{-2} k_B T/a^2$), consistent with the small difference in free energy between the fluid and the crystal phase.

In 2D systems the bulk crystal growth rate was found to decrease due to the presence of impurities [86, 87]. The extent to which the growth rate decreased was larger nearer the impurity, because of the incommensurate nature of the impurity with a crystal structure, further evidenced by a fluid layer of particles surrounding the impurity.

Because of the low interfacial tension between the fluid and crystal phases thermal fluctuations become important and can influence the sharpness of the interface. Studying these effects is relevant to other systems with low surface tension such as biological lipid interfaces.

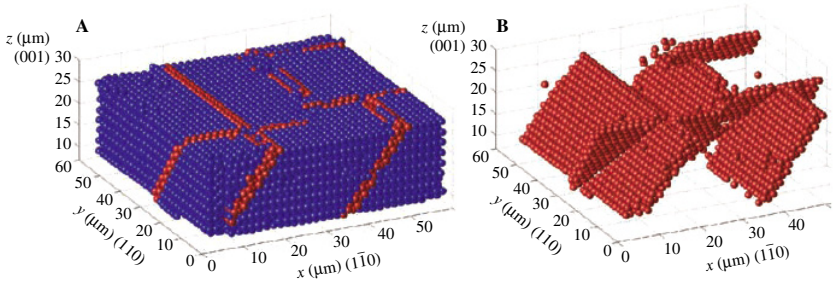

Figure 4. From [89]. Reprinted with permission from AAAS. (A) 3D reconstruction of a 55 μm by 55 μm by 17 μm crystal grown on a template. The red spheres define stacking faults in an otherwise perfect fcc crystal (described by the blue particles). (B) Particles that are adjacent to the stacking fault.

Dullens and co-workers [88] looked at crystal–fluid interfaces under the influence of gravity. This was done by controlling the buoyancy of the colloids and observing the width of the interface. The interface width was quantified by identifying where the colloid number density changed from 10% to 90% of its value in the crystal relative to its value in the fluid phase. Counter-intuitively, they observed the interface to broaden (or become more 'rough') upon increasing the density difference between the particles and the solvent (from 8 to nearly 15 particle diameters in width for $\Delta\rho$ going from 0.024 to 0.256 g ml^{-1}). The explanation for this effect was suggested to be caused by the non-equilibrium nature of the interface. The increased density difference caused the flux of particles arriving at the interface to increase, thereby increasing both the local number density and also the fluctuations. It is anticipated that similar effects may be seen in other interfacial systems such as the gas–fluid interface, and also in systems driven by external forces.

While the above experiments focused on non-equilibrium phenomena, the equilibrium structures of colloidal crystals are also extremely interesting. In particular, they provide insights towards understanding defects and grain boundaries [89, 90] commonly seen in atomic and molecular crystals. Schall and co-workers grew large face-centred cubic (fcc) crystals by sedimenting colloids on a patterned surface [89, 91]. By changing the particle size with respect to the lattice parameter of the surface they were able to create dislocations in the crystal in a controlled manner [89]. A 3D reconstruction of the dislocations can be seen in figure 4. The nearest neighbour configuration was found to be hcp (hexagonal close packed) at the defects, as can be seen in figure 4(B) (in red). The red planes sandwich a stacking fault where the order of the planes changes from ABCABCABC to ABCBCABCA. The authors also showed that the stacking faults culminated in a partial dislocation termed as a Shockley fault, also seen in fcc metals. Therefore, these colloidal crystals were able to capture features seen in continuum systems such as atomic crystals.

While monodisperse hard-sphere crystals are interesting in their own right, binary crystals formed by mixtures of hard spheres [92–94] may also provide unique insights into atomic systems such as alloys. The challenge in such bidisperse systems is to identify both species of particles simultaneously. This can be done with two different fluorescent dyes or image analysis techniques which can identify the two particle sizes separately.

5.2. Hard-sphere colloidal glasses

Colloidal glass was one of the first colloidal phases to be investigated with confocal microscopy [8]. When a glass is formed from a liquid, either by cooling (for an atomic

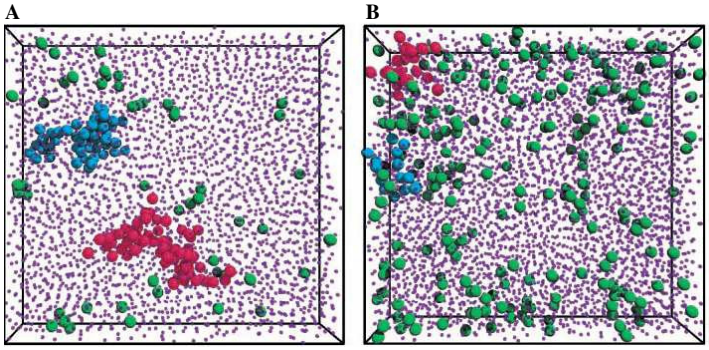

Figure 5. From [99]. Reprinted with permission from AAAS. Three-dimensional rendering of colloidal samples with locations of the fastest moving particles (large spheres) and other particles (smaller spheres), over a fixed time Δt. The samples are (A) supercooled liquid with $\phi = 0.56$ and (B) glassy sample with $\phi = 0.61$. Clearly, in the supercooled fluid, one can see large clusters of fast moving particles (there are 70 red particles clustered together), while these clusters are absent in the glassy sample.

or molecular glass) or by increasing the volume fraction (for a colloidal glass), its viscosity increases by many orders of magnitude. The exact mechanism of this transition, whether thermodynamic or kinetic, is still a matter of debate [26–29]. The consensus in recent years seems to be that the transition, at least for colloidal glasses, is primarily kinetic [95, 96]. One reason for this is that no evidence of a diverging correlation length has been found in the static local structure of glasses [8]. Most theories of the glass transition therefore look at microscopic dynamical mechanisms, the underlying concept of which involves some form of cooperative motion between the molecules or colloids. The arrest of motion at the glass transition is said to be caused by the divergence of the size of these cooperative regions [97].

Several groups [98, 99] used confocal microscopy to try to observe these 'dynamical heterogeneities'. Kegel and co-workers [98] obtained evidence of these spatially heterogeneous dynamics by measuring the van Hove correlation function $G_s(\Delta x, \tau)$ of the particle trajectories. This quantity is the ensemble averaged probability distribution for particle displacements Δx and is therefore a Gaussian for systems such as colloidal suspensions at very dilute ϕ that are purely Brownian. Due to dynamical heterogeneities, however, this quantity is no longer Gaussian for a glass. Kegel *et al* found that $G_s(x, \tau)$ could be described as a sum of two Gaussians—a wide one with fast-moving particles and a narrow one with slower particles [98]—thus obtaining indirect evidence of the presence of domains of differing mobilities.

Weeks *et al* [99] observed the dynamics of both the fast and the slow particles in supercooled colloidal liquids in 3D. In the supercooled phase the motions of the fast-moving particles were strongly correlated spatially in clusters. As the glass transition was approached these domains grew in size, consistent with theoretical predictions of the Adams and Gibbs hypothesis [100]. In the glass phase, however, the average size of these clusters was reduced, providing a dynamic signature of the glass transition. A comparison of the two phases is shown in figure 5 with the fastest particles being represented by large spheres. In the supercooled fluid two large clusters with 50–70 particles each can be seen while the glass has a larger number of small clusters. The mobile particles are weakly correlated with regions of lower density [101, 102], although this is not a strong enough correlation to be predictive of the dynamics in advance [103].

The slowing of the dynamics is often thought of as the confinement of a particle by a cage formed by its neighbours. While light scattering studies have provided indirect evidence of cage motions and rearrangements [104–106], the actual motion of the particles trapped in these cages has been observed only recently [101, 102, 107, 108]. Looking at the *direction* of the particle motion shows that neighbouring particles typically rearrange by moving in parallel directions. A surprisingly non-trivial fraction of neighbouring particles, however, seem to move in antiparallel directions [109]. This is due to pairs of particles moving together to close a gap, often simultaneously with other pairs of particles moving away from the same gap [101]. In other words, four particles at the corner of a square configuration in a plane move about to form a planar diamond configuration.

5.3. Ageing in colloidal glasses

An important difference between supercooled fluids and glasses is their history dependent behaviour: particle motion in a colloidal glass slows down as the sample ages. This is most apparent in the mean square displacement (MSD) of the particles, which can be measured either indirectly, by light scattering or by directly tracking the motions of the particles with confocal microscopy [99, 110]. At short and intermediate lag times the MSD curves of glasses are indistinct from supercooled fluids, exhibiting linear behaviour at short times and a plateau at intermediate times due to confinement by neighbouring particles. At long times, however, the particles break free from their cages, and the MSD curve rises. For supercooled fluids, this increase indicates diffusive motion through the sample, albeit on very slow time scales. An asymptotic diffusion coefficient D_∞ can be determined from these measurements and is independent of the age of the sample [101, 102]. In glasses, however, the upturn indicates only local rearrangements, and the time scale at which the upturn is seen depends on the age of the sample [111]. In older samples the upturn happens at later times and D_∞ is not well defined but rather depends on the age of the sample.

Ageing of colloidal glasses has been studied using confocal microscopy, and it was found that the local rearrangements take place in a spatially heterogeneous fashion [110] similar to that shown in figure 5(A). This differs slightly from the conclusions of [99], which found that the clusters of mobile particles in the glass were small. The key improvement in the data analysis was to average each particle trajectory over time to filter out local Brownian motion and thus more clearly see the slight irreversible rearrangements that cause the sample to age [110]. In the ageing sample, the size of the mobile regions of particles showed no dependence on the age of the glass, a perhaps surprising result. Moreover, spatially heterogeneous motion was found even on time scales significantly shorter than the age of the system. Locally, ageing happens in intermittent bursts with periods of time where the sample does not locally age [110]. This agrees with similar observations from novel light scattering techniques [112].

As the original observations found no link between the length scales of dynamical heterogeneities and the age of the sample, the next confocal studies tried to link changes in local structure to ageing of a glass [113, 114]. Unfortunately, to date no correlations between the age and structure have been found. The physical mechanism for ageing therefore remains an active area of research for many groups.

5.4. Systems under shear

The relationship between the microscopic behaviour of a colloidal suspension and its flow properties is of strong industrial interest. For many materials, the flow properties are characterized through rheology, as discussed in section 3. For example, a dense colloidal

suspension (e.g. toothpaste) is placed between two parallel circular plates and the top plate rotated in an oscillatory fashion while the torque required to cause these oscillations is measured. The relationship between the strain and the stress as a function of frequency is one way to characterize the viscoelastic properties of a sample [32]. This macroscopic methodology has inspired several groups to study the microscopic behaviour of dense colloidal suspensions while they are being sheared.

The application of shear to a colloidal suspension can have a dramatic impact on its microstructure and dynamics. Oscillatory shear applied to a dense monodisperse suspension, for example, results in the spheres forming hexagonally close packed (hcp) layers [115–118] (first observed directly using light scattering and optical microscopy). There are significant challenges to determining the structural and dynamical changes in the suspension when shear is applied, especially for optical methods. Particles subjected to shear rapidly move past the field of view making visualization of individual trajectories difficult. This difficulty can be circumvented in certain cases by imaging immediately after stopping the shear [119]. Another ingenious technique involves a counter-rotating shear cell, with the upper and lower parts of the cell moving in opposite directions, resulting in a stationary plane being formed in the interior. In a cone-plate geometry, for example, the angular velocity ratios of the two components can be tuned to move the stationary plane within the bulk [120]. Other designs involve parallel plates that move in opposite directions with different velocities so that the stationary plane can again be varied as a function of height [121].

Rapid motion of particles out of the field of view has prevented systems under shear from being extensively studied, although fast confocal microscopes provide some hope to address this issue. Colloidal crystals are an exception, since the colloids are locked in to their lattice positions. Derks *et al* [120] used this property to measure the velocity of crystalline particle layers about the zero-shear plane. The shear rate in these layers is much higher than the applied shear; it was postulated that this is due to shear banding effects. The observed region was too small to give direct evidence of this effect, however, which had been previously seen by other indirect measurements [122]. They also observed that the velocity of a crystalline layer was intermediate to its neighbouring two layers. To facilitate the sliding of the layers, the particles performed a zigzag motion which was observed directly, similar to light scattering measurements [122]. More recently, Solomon and Solomon [123] looked at the effects of shear on the stacking faults in colloidal crystals. They observed and quantified non-random spatial heterogeneity in these faults, especially at high amplitudes of strain ($\gamma \geqslant 3$), something not expected by theory.

Other experiments on sheared colloidal crystals look at the effects of confinement on the structures observed [124, 125]. When the gap between the shearing plates is below a critical value and is incommensurate with the crystal structure the crystals break up to form a new ordering. The particles form 'buckled' layers of one, two or three particle bands that are oriented parallel to the shearing direction with fluid voids between these bands. The positions and velocities of these bands depend sensitively on the depth of the particles from the plates.

Recent studies [80, 121] have attempted to look at the effects of shear on non-crystalline glassy suspensions. In the study by Bessling *et al* [121] a fast confocal (VT-Eye, Visitech International) took an entire 3D stack of images within ∼2 s. Relatively small shear rates ($\dot{\gamma} \sim 10^{-3}$ s^{-1}) were employed and so individual particle trajectories could be visualized. Individual particle trajectories showed cage rattling followed by shear-induced plastic cage-breaking events. These plastic, non-affine rearrangements were heterogeneous and seemed to occur cooperatively, similar to rearrangements seen in *quiescent* colloidal suspensions below the glass transition. Further, even though the shear was applied in the z-direction, no anisotropy was found in the diffusion of the colloids.

6. Observations of interacting systems

6.1. Colloidal gels

Attractive interactions between colloids cause them to stick together, and sometimes aggregate to form an elastic solid or gel. The strength of the gel depends sensitively on both the depth and the range of the interparticle interaction. As discussed in section 2.2, there are several causes of attractive interactions. If there are no significant steric or Coulombic interactions, the depth and range of the depletion interaction can be independently controllable. If Coulombic forces are present, adding salt can shrink the size of the Debye double layer, diminishing the repulsion until the colloids aggregate by van der Waals attraction. Sterically stabilized colloids can be cooled from high temperatures, causing the surface grafted polymer layers on the colloid to change conformation, again allowing the colloids to approach close enough to aggregate by the van der Waals attraction.

Gels created by addition of salt typically form at extremely low volume fraction ($\phi \sim 10^{-4}$) with a fractal like structure and fractal clusters of well defined size. The van der Waals attraction is extremely strong, which explains the ability to form such low-ϕ gels. While it takes time for the colloids to approach each other in such a dilute system, once they come close they stick essentially irreversibly. In time, the fractal clusters grow and span the system as a tenuous gel. These gels have been extensively studied with bulk techniques such as light scattering and rheology and the relation between microstructure, dynamics and elastic properties has been elucidated [126–128]. Gels formed by depletion or temperature driven destabilization have weaker attractive forces, and thus a stable gel phase forms at higher volume fractions. The topology of these gels at short length scales below a cluster size becomes important and confocal microscopy provides valuable information on these dense systems.

Dinsmore *et al* [78, 129] have looked at the topology of depletion gels and the effect of changing the range of the depletion interaction on its elasticity. They found that the pair correlation function $g(r)$ displayed power-law behaviour at large r with $g(r) \sim r^{d_f-3}$ where $d_f = 2.1 \pm 0.1$ is the fractal dimension. This was taken to be evidence of the gel consisting of a network of intersecting chains. The contour length L (the shortest path between two particles along the gel) and the number of particles N in the path scale as r^{d_b} with $d_b = 1.2 \pm 0.1$. Since multiple paths can exist between pairs of particles in the gel, the role of loops in the gel elasticity was also probed, by looking at the second shortest non-intersecting path between particles. Unlike in the shortest path, here a difference was found for different ranges of interactions, with short-range interactions creating far fewer loops than longer-range interactions.

The elasticity of *individual* chains was determined by looking at statistics of particle separations and determining the spring constant $\kappa(r)$. The scaling forms of $\kappa(r)$ showed that long-range interactions created chains that resist stress by bond bending while chains created by short-range interactions did so by bond stretching between connected particles. In this way the bulk elasticity of the gels was linked to the microstructure at the particle level.

An intriguing observation in colloidal systems with depletion interactions is the presence of a 'fluid cluster' phase [130–133]. This phase consists of compact clusters of particles (see figure 6) that do not form a network structure or percolate over extended periods of time. The morphology of these clusters is relatively independent of ϕ, but sensitively dependent on the range of the depletion potential [130]. Particles with a longer-range attraction typically had 10–15 neighbours, while those with a shorter-range attraction typically had only three to five neighbours. The internal structure of the clusters revealed a further difference: clusters of particles with long-range interactions had a volume fraction of $\phi \sim 0.46$, while those of particles with short-range interactions did not have a well defined volume fraction due to their

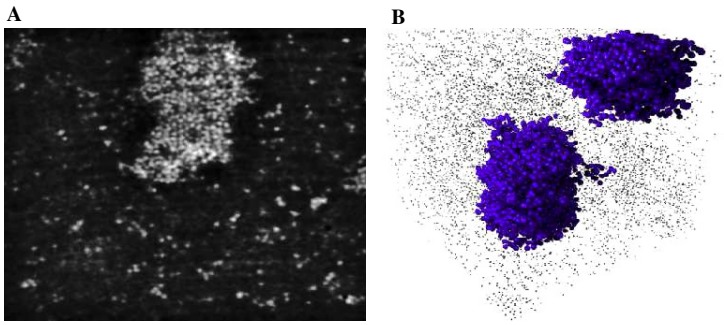

Figure 6. Reprinted with permission from [130]. Copyright 2006 by the American Physical Society. (A) Two-dimensional slice of a fluid cluster phase, where the clusters are in coexistence with individual particles. (B) Three-dimensional reconstruction of (A), where the clusters that appear to be joined together are clearly distinct. The internal volume fraction of the clusters is $\phi = 0.46$, which means they are fairly compact.

fractal nature. Some groups [132, 134, 135] have postulated that these fluid clusters persist due to the presence of charge in these systems. In the absence of any long-range repulsion and the presence of an attractive interaction [130], however, the underlying reason for their existence remains a matter of debate and active research.

In dense colloidal gels the fractal nature of the clusters seen in low volume fraction gels breaks down. Varadan and Solomon [136] found that the overall shape of $g(r)$ for gels with high volume fractions ($\phi > 0.25$) was typical of those seen in dense liquid structures. The heterogeneity in the structure of the gels was determined by measuring the distribution of Voronoi polyhedra volumes of the particles. As ϕ increased, the distribution of these volumes shifted towards lower volumes. Hence, although clusters are absent in these gels, the number density of the particles is redistributed by the creation of voids within the gels.

Recently, a novel means of controlling particle attraction and repulsion, termed nanoparticle haloing, has been found [137, 138]. Strongly charged nanoparticles surround negligibly charged large colloidal particles resulting in a variety of phases. At low nanoparticle concentrations, the large colloidal particles aggregate due to the van der Waals force. At intermediate nanoparticle concentrations the large colloids become coated with the nanoparticles, and effectively charge-stabilized. At high nanoparticle concentrations this stabilization is reversed and the large colloids again flocculate. Confocal microscopy has been used to investigate these phase behaviours [139, 140]. By careful tuning of nanoparticle concentrations, dense or tenuous gels or crystalline phases can be formed [140]. Nanoparticle bridging can modify the gel structure of more strongly charged large particles as well [139].

6.2. Attractive glasses

The glass transition is typically achieved by increasing the packing fraction of colloids. Adding polymer to a dilute hard-sphere colloidal suspension can result in the formation of a gel which is characterized by a freezing of the dynamics. Recently, it was found that adding small amounts of polymer to a colloidal glass caused it to melt with the particles becoming more mobile [141–145]. Further addition of polymer caused the system to re-enter the glassy state, although the arrest in dynamics was now caused by particle bonding (attractive glass), rather than a cage effect of neighbours (repulsive glass). The studies above were performed by light scattering and visual observation, as well as a new technique called coherent anti-Stokes Raman scattering (CARS) microscopy [145], but a recent confocal study [146] has verified

this 'devitrified' glass as well as the return of the glass phase by adding more polymer. It is important to note that there were no significant differences in either structure or local density fluctuations between any of the phases (repulsive glass, devitrifed glass, attractive glass).

6.3. Liquid–liquid or liquid–solid coexistence

As noted in section 2.2, attractive forces are important for modelling real materials. For example, modifying the ideal gas law with a van der Waals attractive force produces a phase transition between a low-density gas state and a high-density liquid state [147]. Adding polymer to a hard-sphere colloidal suspension results in an attractive depletion force which then produces a similar gas/liquid phase transition. These colloid–polymer mixtures can phase separate into coexisting phases of colloid-rich and colloid-poor phases [148]. The colloid-rich phase is either crystalline or fluid in nature [149], depending on the depth and range of the attractive potential, while the colloid-poor domain is always fluid. Fluid–fluid phase separation occurs rapidly followed by slow coarsening of the two phases. While the initial phase separation is too rapid to be observed by confocal microscopy, the subsequent coarsening process follows a three-stage process; interfacial-tension driven coarsening, gravity driven flow and finally interface formation [150]. The shape of the meniscus formed by the interface gives an estimate of the interfacial tension γ between the two fluid phases [151] that is extremely low ($\gamma \sim 0.2\ \mu$N m), especially when compared to fluid–fluid interfaces of molecular liquids (the air–water interfacial tension is of order $\gamma \sim 50$ mN m^{-1}).

The consequence of such low interfacial tension is that thermal fluctuations can create undulations, or roughness, at an interface of order $\sim\sqrt{k_{\mathrm{B}}T/\gamma}$. A density mismatch between the solvent and colloid can also create thermal capillary waves at the interface. The characteristic capillary length $\xi \sim \sqrt{\gamma/g\Delta\rho}$, which is in the μm regime, and the time scale associated with the decay of interfacial fluctuations $\tau \sim \xi\eta/\gamma$ is of the order of seconds for colloidal systems. Hence, these thermal capillary waves can be observed by confocal microscopy, as was done by Aarts and co-workers [152, 153]. Because the colloid-poor region is less intense than the colloid-rich region, the position of the interface, $h(x, t)$ (x is the direction along the interface), can be determined by where the pixel intensity of the images undergoes a sharp transition. By correlating $h(x, t)$ at different values of x and t different modes of the capillary waves were observed that agreed very well with theoretical predictions.

6.4. Ionic systems

For many years the model system for hard-sphere interactions has been PMMA spheres suspended in an index- and density-matching mixture of organic solvents [6]. Recent studies [42] have observed that this system has electrostatic interactions induced by residual charges left on the surface of the PMMA spheres. The organic solvents are polar enough (the dielectric constant is $\varepsilon = 5$–6) that this interaction is fairly long-ranged. The range of the repulsive interactions can be tuned by adding a salt (tetrabutylammonium chloride), and the interactions changed from hard-sphere-like to soft and dipolar. Under certain circumstances, the charge of the colloid can also be changed or reversed from positive to negative at moderate salt concentrations [154].

The effects of the interparticle potential are seen by observing the phase behaviour at varying κa, where κ is the inverse electrostatic screening length and a is the radius of the colloid. For large κa (hard potential), crystals form at high volume fraction ($\phi > 0.545$), and are rhcp in structure. As κa is lowered the fluid-crystal phase boundary shifts to lower ϕ and, further, the structures obtained are fcc for a wide range of κa values. For values of $\kappa a \sim 0.15$

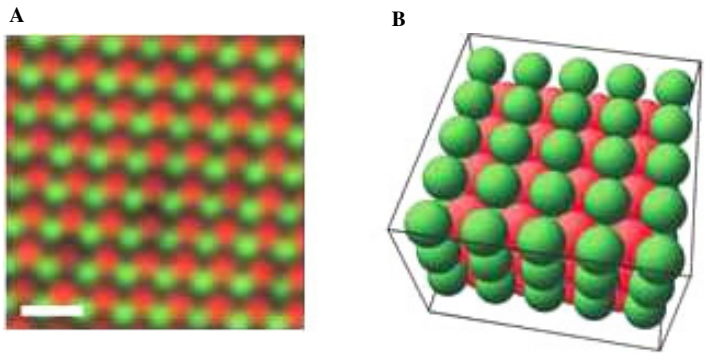

Figure 7. Reprinted with permission from Macmillan Publishers Ltd: [157] copyright 2005. (A) Confocal slice of the (100) plane of a colloidal mixture that forms a CsCl lattice. The red and green spheres represent the two similar sized colloids with opposite charges. The scale bar on the image is 10 μm. (B) Three-dimensional model of what the structure looks like.

crystals form at volume fractions as low as $\phi = 0.002$. (The structures obtained agree with simulations that use a pure Yukawa [155] or hard sphere plus Yukawa potential [155].)

Control of the interparticle potential through ionic charge can be used to form new types of crystalline structure. By mixing colloids of opposite charge large stable *ionic* crystals can be formed that mimic atomic crystals [156–158]. Leunissen and co-workers [157] reproduced the CsCl structure by mixing suspensions of two similar sized spheres ($a \approx 1$ μm) with opposite, equal charges. The CsCl structure (shown in figure 7) consists of two interlaced simple cubic lattices that together form a body centred cubic (bcc) lattice. Changing the size ratio of the particle species with opposing charges had a profound effect on the structures of the ionic crystals formed. By choosing a ratio of 0.31 between the small (S) and large (L) spheres, the authors were able to observe crystals with LS, LS_6 and LS_8 stoichiometry, for varying ionic strengths. Some of these structures (such as NaCl for LS stoichiometry) had analogues with atomic/molecular crystals, while others (LS_8 for example) had no such counterpart. The lattice structures of these crystals, as observed by confocal microscopy, was interesting and non-trivial; a detailed description of the structures can be found in [157]. Future research in this field would entail tailoring structures on demand by tuning size ratios and ionic properties of the colloids.

The presence of charge in colloidal systems, as well as the apolar nature of the solvents, allows for the use of electric fields to manipulate structures and form new phases [42, 159–161]. For instance, both hard-sphere and soft-sphere colloids at low to moderate volume fractions form strings that align in the direction of the applied electric field [42, 159]. These strings were found to be unstable for hard spheres, and began evolving over time to form sheets and body-centred tetragonal (bct) structures [159]. Strings of soft spheres, on the other hand, were stable for extended periods of time. At higher electric fields the dipolar attraction between strings dominated over the charge repulsion between spheres and the strings gave way to form bct crystallites [159]. Other structures observed with soft spheres were bcc and body centred orthogonal structures. A detailed phase diagram of these structures can be found in [42].

Electric fields can also be used to study solid–solid diffusionless or 'martensic' transitions [160]. Dassanayake and co-workers applied increasing electric fields to a close packed (cp) crystal formed by sedimentation, and observed a structural transition from cp to bct as a function of electric field strength, based on a subtle competition between gravity and dipolar attraction. Surprisingly, near the transition threshold, the two phases were found to

coexist for long periods of time. While this raises interesting questions about the order of the phase transition, further studies, similar to those seen in fluid–fluid phase separation, are needed. Finally, these new structures formed by the subtle interplay between attractive forces and repulsion or gravity, while having interesting physics, also have great application such as in photonic band gap structures.

6.5. Anisotropic systems

While attractive and repulsive interactions help make colloids better models for atomic systems, the systems described above lack one interesting feature: the interactions are all spherically symmetric. With improving synthesis techniques, several groups now study the phase behaviour of non-spherical colloidal particles. Confocal microscopy has been used to characterize samples consisting of non-spherical colloids such as polyhedra [162] or anisotropic ones such as dumbbells [163] and rods [164, 165].

It is crucial but non-trivial to identify the orientation of these anisotropic colloids in a confocal image. Colloidal dumbbells [163] consist of dimers of silica spheres that have been fused together. It is difficult to resolve these dumbbells using x-ray scattering except at high scattering wavenumbers. However, because the distance between two spheres that are part of the same dumbbell is less than any other separation between spheres in the sample, dumbbells can be identified by measuring the distance between the fluorescent core centres of the silica particles. Using these identified centres, the position and orientation of all the dumbbells in a 3D sample could be measured. A similar problem exists for the case of colloidal rods [164], made by uniaxially extending PMMA spheres. In this case an algorithm was devised to identify the backbones of the rods, therefore associating a central axis with each rod. The centroid of the rod was determined by averaging the pixel positions of the points comprising this central axis, and the rod was characterized by its length and orientation. This technique worked remarkably well even for highly concentrated, nearly close packed rods.

Confocal microscopy has also been used to characterize non-spherical 'polyhedral' colloids [162], where the particle shape is characterized by comparing the projected particle area in 2D to its projected perimeter. The close packing of the particles showed deviations from those of spherical particles. Especially interesting was the fact that $g(r)$ decayed much faster for polyhedral colloids than spheres, implying no long-range translational order. The bond-orientational correlation function $g_6(r)$ also decayed faster, implying frustration of hexagonal order in these polyhedra. Conceivably, with advances in particle synthesis and new types of particles being produced with ease, confocal microscopy can have great application in determining unique structures and phases these particles may form, especially because of the ease of 3D reconstruction.

7. New directions

In this review we have tried to touch upon many aspects of the phase behaviour of colloids that interact either as hard spheres or with repulsive/attractive potentials. Apart from these well-studied systems with thermodynamic analogies to atomic and molecular systems [166], colloids have other applications as well. For instance, they are used as tracer particles in viscoelastic solutions to probe the rheological properties of the environment around them. For spatially heterogeneous materials, confocal microscopy of the thermal motions of these particles in three dimensions can be very useful [167, 168]. Further, the effects of shear on these viscoelastic materials can also be probed [168].

Large colloids, such as emulsion droplets, can also be used to mimic granular systems. Emulsions are visualized either by dying the dispersed phase [169, 170] or by utilizing

fluorescent surfactants that go to the interface between the dispersed phase and the continuous phase [171]. The force between two droplets that are in contact can be quantified by characterizing the shape of these compressible droplets [169, 171, 172]. Thus a spatial distribution of 'force chains' in three dimensions can be obtained, which has analogies with such chains seen in granular materials.

In conclusion, colloidal systems show behaviour than spans the gamut from atomic systems (with length and time scales in the nanometre and picosecond range) to granular materials (millimetres and seconds). Confocal microscopy is key to the observation of these phenomena in real space and real time, and this powerful technique holds much promise for future research.

Acknowledgments

We thank Scott V Franklin and G C Cianci for enlightening discussions. E R Weeks and V Prasad thank NSF (DMR-0239109) for funding.

References

[1] Habdas P and Weeks E R 2002 Video microscopy of colloidal suspensions and colloidal crystals *Curr. Opin. Colloid Interface Sci.* **7** 196–203
[2] Minsky M 1988 Memoir on inventing the confocal scanning microscope *Scanning* **10** 128–38
[3] Sheppard C J R and Shotton D M 1997 *Confocal Laser Scanning Microscopy* (New York: Springer)
[4] Inoué S and Spring K R 1997 *Video Microscopy: The Fundamentals* (New York: Plenum)
[5] Pawley J B 1995 *Handbook of Biological Confocal Microscopy* (New York: Plenum)
[6] Pusey P N and van Megen W 1986 Phase-behavior of concentrated suspensions of nearly hard colloidal spheres *Nature* **320** 340–2
[7] Yoshida H, Ito K and Ise N 1991 Localized ordered structure in polymer latex suspensions as studied by a confocal laser scanning microscope *Phys. Rev.* B **44** 435–8
[8] van Blaaderen A and Wiltzius P 1995 Real-space structure of colloidal hard-sphere glasses *Science* **270** 1177–9
[9] Alder B J and Wainwright T E 1970 Decay of velocity autocorrelation function *Phys. Rev.* A **1** 18–21
[10] Woodcock L V 1981 Glass-transition in the hard-sphere model and Kauzmann paradox *Ann. NY Acad. Sci.* **371** 274–98
[11] Speedy R J 1998 The hard sphere glass transition *Mol. Phys.* **95** 169–78
[12] Alder B J, Gass D M and Wainwright T E 1970 Studies in molecular dynamics.8. transport coefficients for a hard-sphere fluid *J. Chem. Phys.* **53** 3813–26
[13] Alder B J and Wainwright T E 1957 Phase transition for a hard sphere system *J. Chem. Phys.* **27** 1208–9
[14] Zhu J X, Li M, Rogers R, Meyer W, Ottewill R H, Russell W B and Chaikin P M 1997 Crystallization of hard-sphere colloids in microgravity *Nature* **387** 883–5
[15] Hoogenboom J P, Vergeer P and van Blaaderen A 2003 A real-space analysis of colloidal crystallization in a gravitational field at a flat bottom wall *J. Chem. Phys.* **119** 3371–83
[16] Royall C P, van Roij R and van Blaaderen A 2005 Extended sedimentation profiles in charged colloids: the gravitational length, entropy, and electrostatics *J. Phys.: Condens. Matter* **17** 2315–26
[17] Simeonova N B and Kegel W K 2004 Gravity-induced aging in glasses of colloidal hard spheres *Phys. Rev. Lett.* **93** 035701
[18] Bernal J D 1959 Geometrical approach to the structure of liquids *Nature* **183** 141–7
[19] Bernal J D 1960 Geometry of the structure of monatomic liquids *Nature* **185** 68–70
[20] Bernal J D 1964 Bakerian lecture 1962—structure of liquids *Proc. R. Soc.* A **280** 299
[21] Torquato S, Truskett T M and Debenedetti P G 2000 Is random close packing of spheres well defined? *Phys. Rev. Lett.* **84** 2064–7
[22] Moriguchi I, Kawasaki K and Kawakatsu T 1993 The effects of size polydispersity in nearly hard-sphere colloids *J. Physique* II **3** 1179–84
[23] Williams S R, Snook I K and van Megen W 2001 Molecular dynamics study of the stability of the hard sphere glass *Phys. Rev.* E **6402** 021506
[24] Cheng Z D, Zhu J X, Chaikin P M, Phan S E and Russel W B 2002 Nature of the divergence in low shear viscosity of colloidal hard-sphere dispersions *Phys. Rev.* E **65** 041405
[25] Pusey P N 1991 *Liquids, Freezing and the Glass Transition* (Amsterdam: Elsevier)

[26] Angell C A 1995 Formation of glasses from liquids and biopolymers *Science* **267** 1924–35
[27] Angell C A 2000 Ten questions on glassformers, and a real space 'excitations' model with some answers on fragility and phase transitions *J. Phys.: Condens. Matter* **12** 6463–75
[28] Stillinger F H 1995 A topographic view of supercooled liquids and glass-formation *Science* **267** 1935–9
[29] Ediger M D, Angell C A and Nagel S R 1996 Supercooled liquids and glasses *J. Phys. Chem.* **100** 13200–12
[30] Russel W B, Saville D A and Schowalter W R 1989 *Colloidal Dispersions* (Cambridge: Cambridge University Press)
[31] Jones R A L 2002 *Soft Condensed Matter* (Oxford: Oxford University Press)
[32] Larson R G 1998 *The Structure and Rheology of Complex Fluids* (Oxford: Oxford University Press)
[33] Antl L, Goodwin J W, Hill R D, Ottewill R H, Owens S M, Papworth S and Waters J A 1986 The preparation of poly(methyl methacrylate) lattices in nonaqueous media *Colloids Surf.* **17** 67–78
[34] Pusey P N, van Megen W, Bartlett P, Ackerson B J, Rarity J G and Underwood S M 1989 Structure of crystals of hard colloidal spheres *Phys. Rev. Lett.* **63** 2753–6
[35] Asakura S and Oosawa F 1958 Interaction between particles suspended in solutions of macromolecules *J. Polym. Sci.* **33** 183–92
[36] Crocker J C, Matteo J A, Dinsmore A D and Yodh A G 1999 Entropic attraction and repulsion in binary colloids probed with a line optical tweezer *Phys. Rev. Lett.* **82** 4352–5
[37] Verma R, Crocker J C, Lubensky T C and Yodh A G 2000 Attractions between hard colloidal spheres in semiflexible polymer solutions *Macromolecules* **33** 177–86
[38] Bosma G, Pathmamanoharan C, de Hoog E H A, Kegel W K, van Blaaderen A and Lekkerkerker H N W 2002 Preparation of monodisperse, fluorescent pmma-latex colloids by dispersion polymerization *J. Colloid Interface Sci.* **245** 292–300
[39] Dullens R P A, Claesson M, Derks D, van Blaaderen A and Kegel W K 2003 Monodisperse core-shell poly(methyl methacrylate) latex colloids *Langmuir* **19** 5963–6
[40] Campbell A I and Bartlett P 2002 Fluorescent hard-sphere polymer colloids for confocal microscopy *J. Colloid Interface Sci.* **256** 325–30
[41] van Blaaderen A and Vrij A 1992 Synthesis and characterization of colloidal dispersions of fluorescent, monodisperse silica spheres *Langmuir* **8** 2921–31
[42] Yethiraj A and van Blaaderen A 2003 A colloidal model system with an interaction tunable from hard sphere to soft and dipolar *Nature* **421** 513–7
[43] Stieger M, Richtering W, Pedersen J S and Lindner P 2004 Small-angle neutron scattering study of structural changes in temperature sensitive microgel colloids *J. Chem. Phys.* **120** 6197–206
[44] Ye X, Narayanan T, Tong P, Huang J S, Lin M Y, Carvalho B L and Fetters L J 1996 Depletion interactions in colloid-polymer mixtures *Phys. Rev.* E **54** 6500–10
[45] Ye X, Narayanan T and Tong P 1996 Neutron scattering study of depletion interactions in a colloid-polymer mixture *Phys. Rev. Lett.* **76** 4640–3
[46] Ottewill R H, Hanley H J M, Rennie A R and Straty G C 1995 Small-angle neutron-scattering studies on binary-mixtures of charged-particles *Langmuir* **11** 3757–65
[47] Ashdown S, Markovic I, Ottewill R H, Lindner P, Oberthur R C and Rennie A R 1990 Small-angle neutron-scattering studies on ordered polymer colloid dispersions *Langmuir* **6** 303–7
[48] Lal J, Abernathy D, Auvray L, Diat O and Grubel G 2001 Dynamics and correlations in magnetic colloidal systems studied by x-ray photon correlation spectroscopy *Eur. Phys. J.* E **4** 263–71
[49] Konishi T, Yamahara E and Ise N 1996 Characterization of colloidal silica particles by ultra-small-angle x-ray scattering *Langmuir* **12** 2608–10
[50] Dierker S B, Pindak R, Fleming R M, Robinson I K and Berman L 1995 X-ray photon-correlation spectroscopy study of Brownian-motion of gold colloids in glycerol *Phys. Rev. Lett.* **75** 449–52
[51] Konishi T, Ise N, Matsuoka H, Yamaoka H, Sogami I S and Yoshiyama T 1995 Structural study of silica particle dispersions by ultra-small-angle x-ray-scattering *Phys. Rev.* B **51** 3914–7
[52] van Megen W, Underwood S M and Pusey P N 1991 Dynamics of hard spherical colloids from the fluid to the glass *J. Chem. Soc.-Faraday Trans.* **87** 395–401
[53] van Megen W and Pusey P N 1991 Dynamic light-scattering study of the glass-transition in a colloidal suspension *Phys. Rev.* A **43** 5429–41
[54] Carpineti M and Giglio M 1992 Spinodal-type dynamics in fractal aggregation of colloidal clusters *Phys. Rev. Lett.* **68** 3327–30
[55] Dhont J K G, Smits C and Lekkerkerker H N W 1992 A time resolved static light-scattering study on nucleation and crystallization in a colloidal system *J. Colloid Interface Sci.* **152** 386–401
[56] Cipelletti L, Manley S, Ball R C and Weitz D A 2000 Universal aging features in the restructuring of fractal colloidal gels *Phys. Rev. Lett.* **84** 2275–8

[57] Moussaid A and Pusey P N 1999 Multiple scattering suppression in static light scattering by cross-correlation spectroscopy *Phys. Rev.* E **60** 5670–6
[58] Segre P N, van Megen W, Pusey P N, Schatzel K and Peters W 1995 2-color dynamic light-scattering *J. Mod. Opt.* **42** 1929–52
[59] Stieber F and Richtering W 1995 Fiber-optic-dynamic-light-scattering and two-color-cross-correlation studies of turbid, concentrated, sterically stabilized polystyrene latex *Langmuir* **11** 4724–7
[60] Schatzel K, Drewel M and Ahrens J 1990 Suppression of multiple-scattering in photon-correlation spectroscopy *J. Phys.: Condens. Matter* **2** (Suppl. A.) SA393–8
[61] Dasgupta B R, Tee S Y, Crocker J C, Frisken B J and Weitz D A 2002 Microrheology of polyethylene oxide using diffusing wave spectroscopy and single scattering *Phys. Rev.* E **65** 051505
[62] Durian D J, Weitz D A and Pine D J 1990 Dynamics and coarsening in 3-dimensional foams *J. Phys.: Condens. Matter* **2** (Suppl. A.) SA433–6
[63] Pine D J, Weitz D A, Zhu J X and Herbolzheimer E 1990 Diffusing-wave spectroscopy—dynamic light-scattering in the multiple-scattering limit *J. Physique* **51** 2101–27
[64] Pine D J, Weitz D A, Chaikin P M and Herbolzheimer E 1988 Diffusing-wave spectroscopy *Phys. Rev. Lett.* **60** 1134–7
[65] Trappe V, Prasad V, Cipelletti L, Segre P N and Weitz D A 2001 Jamming phase diagram for attractive particles *Nature* **411** 772–5
[66] Trappe V and Weitz D A 2000 Scaling of the viscoelasticity of weakly attractive particles *Phys. Rev. Lett.* **85** 449–52
[67] Fagan M E and Zukoski C F 1997 The rheology of charge stabilized silica suspensions *J. Rheol.* **41** 373–97
[68] Mason T G and Weitz D A 1995 Linear viscoelasticity of colloidal hard-sphere suspensions near the glass-transition *Phys. Rev. Lett.* **75** 2770–3
[69] Gisler T, Ball R and Weitz D A 1999 Strain hardening of fractal colloidal gels *Phys. Rev. Lett.* **82** 1064–7
[70] Prasad V, Trappe V, Dinsmore A D, Segre P N, Cipelletti L and Weitz D A 2003 Universal features of the fluid to solid transition for attractive colloidal particles *Faraday Discuss.* **123** 1–12
[71] Zernike F 1942 Phase contrast, a new method for the microsopic observation of transparent objects *Physica* **9** 686–98
[72] Zernike F 1942 Phase contrast, a new method for the microscopic observation of transparent objects part II *Physica* **9** 974–86
[73] Nomarski M G 1955 Microinterféromètre différentiel à ondes polarisées *J. Physique Radium* **16** (Suppl. S) S9–13
[74] Elliot M S and Poon W C K 2001 Conventional optical microscopy of colloidal suspensions *Adv. Colloid Interface Sci.* **92** 133–94
[75] Baumgartl J, Arauz-Lara J L and Bechinger C 2006 Like-charge attraction in confinement: myth or truth? *Soft Matter* **2** 631–5
[76] Xiao G Q, Corle T R and Kino G S 1988 Real-time confocal scanning optical microscope *Appl. Phys. Lett.* **53** 716–8
[77] Crocker J C and Grier D G 1996 Methods of digital video microscopy for colloidal studies *J. Colloid Interface Sci.* **179** 298–310
[78] Dinsmore A D, Weeks E R, Prasad V, Levitt A C and Weitz D A 2001 Three-dimensional confocal microscopy of colloids *Appl. Opt.* **40** 4152–9
[79] A tutorial on particle tracking can be found at http://www.physics.emory.edu/∼weeks/idl
[80] Isa L, Besseling R, Weeks E R and Poon W C K 2006 Experimental studies of the flow of concentrated hard sphere suspensions into a constriction *J. Phys. Conf. Ser.* **40** 124–32
[81] Nelson D R 2002 *Defects and Geometry in Condensed Matter Physics* (Cambridge: Cambridge University Press)
[82] ten Wolde P R, Ruiz-Montero M J and Frenkel D 1999 Numerical calculation of the rate of homogeneous gas–liquid nucleation in a Lennard-Jones system *J. Chem. Phys.* **110** 1591–9
[83] Steinhardt P J, Nelson D R and Ronchetti M 1983 Bond-orientational order in liquids and glasses *Phys. Rev.* B **28** 784–805
[84] Gasser U, Weeks E R, Schofield A, Pusey P N and Weitz D A 2001 Real-space imaging of nucleation and growth in colloidal crystallization *Science* **292** 258–62
[85] Auer S and Frenkel D 2001 Prediction of absolute crystal-nucleation rate in hard-sphere colloids *Nature* **409** 1020–3
[86] de Villeneuve V W A, Dullens R P A, Aarts D G A L, Groeneveld E, Scherff J H, Kegel W K and Lekkerkerker H N W 2005 Colloidal hard-sphere crystal growth frustrated by large spherical impurities *Science* **309** 1231–3

[87] de Villeneuve V W A, Verboekend D, Dullens R P A, Aarts D G A L, Kegel W K and Lekkerkerker H N W 2005 Hard sphere crystal nucleation and growth near large spherical impurities *J. Phys.: Condens. Matter* **17** (Sp. Iss. SI) S3371–8
[88] Dullens R P A, Aarts D G A L and Kegel W K 2006 Dynamic broadening of the crystal–fluid interface of colloidal hard spheres *Phys. Rev. Lett.* **97** 228301
[89] Schall P, Cohen I, Weitz D A and Spaepen F 2004 Visualization of dislocation dynamics in colloidal crystals *Science* **305** 1944–8
[90] Schall P, Cohen I, Weitz D A and Spaepen F 2006 Visualizing dislocation nucleation by indenting colloidal crystals *Nature* **440** 319–23
[91] Lin K H, Crocker J C, Prasad V, Schofield A, Weitz D A, Lubensky T C and Yodh A G 2000 Entropically driven colloidal crystallization on patterned surfaces *Phys. Rev. Lett.* **85** 1770–3
[92] Hunt N, Jardine R and Bartlett P 2000 Superlattice formation in mixtures of hard-sphere colloids *Phys. Rev.* E **62** 900–13
[93] Schofield A B 2001 Binary hard-sphere crystals with the cesium chloride structure *Phys. Rev.* E **6405** 051403
[94] Bartlett P, Ottewill R H and Pusey P N 1992 Superlattice formation in binary-mixtures of hard-sphere colloids *Phys. Rev. Lett.* **68** 3801–4
[95] Gotze W and Sjogren L 1992 Relaxation processes in supercooled liquids *Rep. Prog. Phys.* **55** 241–376
[96] Bengtzelius U, Gotze W and Sjolander A 1984 Dynamics of supercooled liquids and the glass-transition *J. Phys. C: Solid State Phys.* **17** 5915–34
[97] Ediger M D 2000 Spatially heterogeneous dynamics in supercooled liquids *Annu. Rev. Phys. Chem.* **51** 99–128
[98] Kegel W K and van Blaaderen A 2000 Direct observation of dynamical heterogeneities in colloidal hard-sphere suspensions *Science* **287** 290–3
[99] Weeks E R, Crocker J C, Levitt A C, Schofield A and Weitz D A 2000 Three-dimensional direct imaging of structural relaxation near the colloidal glass transition *Science* **287** 627–31
[100] Adam G and Gibbs J H 1965 On temperature dependence of cooperative relaxation properties in glass-forming liquids *J. Chem. Phys.* **43** 139
[101] Weeks E R and Weitz D A 2002 Properties of cage rearrangements observed near the colloidal glass transition *Phys. Rev. Lett.* **89** 095704
[102] Weeks E R and Weitz D A 2002 Subdiffusion and the cage effect studied near the colloidal glass transition *Chem. Phys.* **284** (Sp. Iss. SI) 361–7
[103] Conrad J C, Starr F W and Weitz D A 2005 Weak correlations between local density and dynamics near the glass transition *J. Phys. Chem.* B **109** 21235–40
[104] Pusey P N and van Megen W 1987 Observation of a glass-transition in suspensions of spherical colloidal particles *Phys. Rev. Lett.* **59** 2083–6
[105] van Megen W, Mortensen T C, Williams S R and Muller J 1998 Measurement of the self-intermediate scattering function of suspensions of hard spherical particles near the glass transition *Phys. Rev.* E **58** 6073–85
[106] van Megen W, Underwood S M and Pusey P N 1991 Nonergodicity parameters of colloidal glasses *Phys. Rev. Lett.* **67** 1586–9
[107] Kasper A, Bartsch E and Sillescu H 1998 Self-diffusion in concentrated colloid suspensions studied by digital video microscopy of core-shell tracer particles *Langmuir* **14** 5004–10
[108] Marcus A H, Schofield J and Rice S A 1999 Experimental observations of non-Gaussian behavior and stringlike cooperative dynamics in concentrated quasi-two-dimensional colloidal liquids *Phys. Rev.* E **60** 5725–36
[109] Weeks E R, Crocker J C and Weitz D A 2006 *Preprint* cond-mat/0610195
[110] Courtland R E and Weeks E R 2003 Direct visualization of ageing in colloidal glasses *J. Phys.: Condens. Matter* **15** (Sp. Iss. SI) S359–65
[111] Henderson S I and van Megen W 1998 Metastability and crystallization in suspensions of mixtures of hard spheres *Phys. Rev. Lett.* **80** 877–80
[112] Cipelletti L, Bissig H, Trappe V, Ballesta P and Mazoyer S 2003 Time-resolved correlation: a new tool for studying temporally heterogeneous dynamics *J. Phys.: Condens. Matter* **15** (Sp. Iss. SI) S257–62
[113] Cianci G C, Courtland R E and Weeks E R 2006 *2nd Int. Conf. on Flow Dynamics*, *AIP Conf. Proc.* **832** 21–5
[114] Cianci G C, Courtland R E and Weeks E R 2006 Correlations of structure and dynamics in an aging colloidal glass *Solid State Commun.* **139** 599–604
[115] Paulin S E, Ackerson B J and Wolfe M S 1997 Microstructure-dependent viscosity in concentrated suspensions of soft spheres *Phys. Rev.* E **55** 5812–9
[116] Ackerson B J and Pusey P N 1988 Shear-induced order in suspensions of hard-spheres *Phys. Rev. Lett.* **61** 1033–6

[117] Haw M D, Poon W C K and Pusey P N 1998 Direct observation of oscillatory-shear-induced order in colloidal suspensions *Phys. Rev.* E **57** 6859–64
[118] Haw M D, Poon W C K, Pusey P N, Hebraud P and Lequeux F 1998 Colloidal glasses under shear strain *Phys. Rev.* E **58** 4673–82
[119] Varadan P and Solomon M J 2003 Direct visualization of flow-induced microstructure in dense colloidal gels by confocal laser scanning microscopy *J. Rheol.* **47** 943–68
[120] Derks D, Wisman H, van Blaaderen A and Imhof A 2004 Confocal microscopy of colloidal dispersions in shear flow using a counter-rotating cone-plate shear cell *J. Phys.: Condens. Matter* **16** (Sp. Iss. SI) S3917–27
[121] Besseling R, Weeks E R, Schofield A B and Poon W C K 2006 *Preprint* cond-mat/0605247
[122] Ackerson B J 1990 Shear induced order and shear processing of model hard-sphere suspensions *J. Rheol.* **34** 553–90
[123] Solomon T and Solomon M J 2006 Stacking fault structure in shear-induced colloidal crystallization *J. Chem. Phys.* **124** 134905
[124] Cohen I, Mason T G and Weitz D A 2004 Shear-induced configurations of confined colloidal suspensions *Phys. Rev. Lett.* **93** 046001
[125] Cohen I, Davidovitch B, Schofield A B, Brenner M P and Weitz D A 2006 Slip, yield, and bands in colloidal crystals under oscillatory shear *Phys. Rev. Lett.* **97** 215502
[126] Ball R C, Weitz D A, Witten T A and Leyvraz F 1987 Universal kinetics in reaction-limited aggregation *Phys. Rev. Lett.* **58** 274–7
[127] Lin M Y, Lindsay H M, Weitz D A, Ball R C, Klein R and Meakin P 1990 Universal reaction-limited colloid aggregation *Phys. Rev.* A **41** 2005–20
[128] Weitz D A and Oliveria M 1984 Fractal structures formed by kinetic aggregation of aqueous gold colloids *Phys. Rev. Lett.* **52** 1433–6
[129] Dinsmore A D and Weitz D A 2002 Direct imaging of three-dimensional structure and topology of colloidal gels *J. Phys.: Condens. Matter* **14** 7581–97
[130] Lu P J, Conrad J C, Wyss H M, Schofield A B and Weitz D A 2006 Fluids of clusters in attractive colloids *Phys. Rev. Lett.* **96** 028306
[131] Segre P N, Prasad V, Schofield A B and Weitz D A 2001 Glasslike kinetic arrest at the colloidal-gelation transition *Phys. Rev. Lett.* **86** 6042–5
[132] Sedgwick H, Egelhaaf S U and Poon W C K 2004 Clusters and gels in systems of sticky particles *J. Phys.: Condens. Matter* **16** (Sp. Iss. SI) S4913–22
[133] Campbell A I, Anderson V J, van Duijneveldt J S and Bartlett P 2005 Dynamical arrest in attractive colloids: the effect of long-range repulsion *Phys. Rev. Lett.* **94** 208301
[134] Groenewold J and Kegel W K 2001 Anomalously large equilibrium clusters of colloids *J. Phys. Chem.* B **105** 11702–9
[135] Groenewold J and Kegel W K 2004 Colloidal cluster phases, gelation and nuclear matter *J. Phys.: Condens. Matter* **16** (Sp. Iss. SI) S4877–86
[136] Varadan P and Solomon M J 2003 Direct visualization of long-range heterogeneous structure in dense colloidal gels *Langmuir* **19** 509–12
[137] Tohver V, Smay J E, Braem A, Braun P V and Lewis J A 2001 Nanoparticle halos: a new colloid stabilization mechanism *Proc. Natl Acad. Sci. USA* **98** 8950–4
[138] Tohver V, Chan A, Sakurada O and Lewis J A 2001 Nanoparticle engineering of complex fluid behavior *Langmuir* **17** 8414–21
[139] Gilchrist J F, Chan A T, Weeks E R and Lewis J A 2005 Phase behavior and 3d structure of strongly attractive microsphere-nanoparticle mixtures *Langmuir* **21** 11040–7
[140] Martinez C J, Liu J W, Rhodes S K, Luijten E, Weeks E R and Lewis J A 2005 Interparticle interactions and direct imaging of colloidal phases assembled from microsphere-nanoparticle mixtures *Langmuir* **21** 9978–89
[141] Pham K N, Egelhaaf S U, Pusey P N and Poon W C K 2004 Glasses in hard spheres with short-range attraction *Phys. Rev.* E **69** 011503
[142] Pham K N, Puertas A M, Bergenholtz J, Egelhaaf S U, Moussaid A, Pusey P N, Schofield A B, Cates M E, Fuchs M and Poon W C K 2002 Multiple glassy states in a simple model system *Science* **296** 104–6
[143] Poon W C K, Pham K N, Egelhaaf S U and Pusey P N 2003 'Unsticking' a colloidal glass, and sticking it again *J. Phys.: Condens. Matter* **15** (Sp. Iss. SI) S269–75
[144] Dawson K A 2002 The glass paradigm for colloidal glasses, gels, and other arrested states driven by attractive interactions *Curr. Opin. Colloid Interface Sci.* **7** 218–27
[145] Kaufman L J and Weitz D A 2006 Direct imaging of repulsive and attractive colloidal glasses *J. Chem. Phys.* **125** 074716

[146] Simeonova N B, Dullens R P A, Aarts D G A L, de Villeneuve V W A, Lekkerkerker H N W and Kegel W K 2006 Devitrification of colloidal glasses in real space *Phys. Rev.* E **73** 041401
[147] Schroeder D V 1999 *An Introduction to Thermal Physics* (Reading, MA: Addison-Wesley)
[148] Ilett S M, Orrock A, Poon W C K and Pusey P N 1995 Phase-behavior of a model colloid-polymer mixture *Phys. Rev.* E **51** 1344–52
[149] de Hoog E H A, Kegel W K, van Blaaderen A and Lekkerkerker H N W 2001 Direct observation of crystallization and aggregation in a phase-separating colloid-polymer suspension *Phys. Rev.* E **6402** 021407
[150] Aarts D G A L, Dullens R P A and Lekkerkerker H N W 2005 Interfacial dynamics in demixing systems with ultralow interfacial tension *New J. Phys.* **7** 40
[151] Aarts D G A L 2005 Capillary length in a fluid–fluid demixed colloid-polymer mixture *J. Phys. Chem.* B **109** 7407–11
[152] Aarts D G A L, Schmidt M and Lekkerkerker H N W 2004 Direct visual observation of thermal capillary waves *Science* **304** 847–50
[153] Aarts D G A L 2007 The interface in demixed colloid-polymer systems: wetting, waves and droplets *Soft Matter* **3** 19–23
[154] Royall C P, Leunissen M E and van Blaaderen A 2003 A new colloidal model system to study long-range interactions quantitatively in real space *J. Phys.: Condens. Matter* **15** (Sp. Iss. SI) S3581–96
[155] Robbins M O, Kremer K and Grest G S 1988 Phase-diagram and dynamics of Yukawa systems *J. Chem. Phys.* **88** 3286–312
[156] Hynninen A P, Leunissen M E, van Blaaderen A and Dijkstra M 2006 Cu Au structure in the restricted primitive model and oppositely charged colloids *Phys. Rev. Lett.* **96** 018303
[157] Leunissen M E, Christova C G, Hynninen A P, Royall C P, Campbell A I, Imhof A, Dijkstra M, van Roij R and van Blaaderen A 2005 Ionic colloidal crystals of oppositely charged particles *Nature* **437** 235–40
[158] Bartlett P and Campbell A I 2005 Three-dimensional binary superlattices of oppositely charged colloids *Phys. Rev. Lett.* **95** 128302
[159] Yethiraj A and van Blaaderen A 2002 Monodisperse colloidal suspensions of silica and PMMA spheres as model electrorheological fluids: a real-space study of structure formation *Int. J. Mod. Phys.* B **16** (Sp. Iss. SI) 2328–33
[160] Yethiraj A, Wouterse A, Groh B and van Blaaderen A 2004 Nature of an electric-field-induced colloidal martensitic transition *Phys. Rev. Lett.* **92** 058301
[161] Dassanayake U, Fraden S and van Blaaderen A 2000 Structure of electrorheological fluids *J. Chem. Phys.* **112** 3851–8
[162] Dullens R P A, Mourad M C D, Aarts D G A L, Hoogenboom J P and Kegel W K 2006 Shape-induced frustration of hexagonal order in polyhedral colloids *Phys. Rev. Lett.* **96** 028304
[163] Johnson P M, van Kats C M and van Blaaderen A 2005 Synthesis of colloidal silica dumbbells *Langmuir* **21** 11510–7
[164] Mohraz A and Solomon M J 2005 Direct visualization of colloidal rod assembly by confocal microscopy *Langmuir* **21** 5298–306
[165] van Kats C M, Johnson P M, van den Meerakker J and van Blaaderen A 2004 Synthesis of monodisperse high-aspect-ratio colloidal silicon and silica rods *Langmuir* **20** 11201–7
[166] Dullens R P A, Aarts D G A L and Kegel W K 2006 Direct measurement of the free energy by optical microscopy *Proc. Natl Acad. Sci. USA* **103** 529–31
[167] Moschakis T, Murray B S and Dickinson E 2006 Particle tracking using confocal microscopy to probe the microrheology in a phase-separating emulsion containing nonadsorbing polysaccharide *Langmuir* **22** 4710–9
[168] Vossen D L J, van der Horst A, Dogterom M and van Blaaderen A 2004 Optical tweezers and confocal microscopy for simultaneous three-dimensional manipulation and imaging in concentrated colloidal dispersions *Rev. Sci. Instrum.* **75** 2960–70
[169] Brujic J, Edwards S F, Grinev D V, Hopkinson I, Brujic D and Makse H A 2003 3d bulk measurements of the force distribution in a compressed emulsion system *Faraday Discuss.* **123** 207–20
[170] Penfold R, Watson A D, Mackie A R and Hibberd D J 2006 Quantitative imaging of aggregated emulsions *Langmuir* **22** 2005–15
[171] Zhou J, Long S, Wang Q and Dinsmore A D 2006 Measurement of forces inside a three-dimensional pile of frictionless droplets *Science* **312** 1631–3
[172] Brujic J, Edwards S F, Hopkinson I and Makse H A 2003 Measuring the distribution of interdroplet forces in a compressed emulsion system *Physica* A **327** 201–12